Interactions of the antiviral and antiparkinson agent amantadine with lipid membranes and human erythrocytes

ARTICLE *in* BIOPHYSICAL CHEMISTRY · JULY 2015

Impact Factor: 1.99 · DOI: 10.1016/j.bpc.2015.04.002

6 AUTHORS, INCLUDING:

Mario Suwalsky
University of Concepción
135 PUBLICATIONS **1,643** CITATIONS
SEE PROFILE

Malgorzata Jemiola-Rzeminska
Jagiellonian University
34 PUBLICATIONS **398** CITATIONS
SEE PROFILE

Kazimierz Strzalka
Jagiellonian University
197 PUBLICATIONS **3,249** CITATIONS
SEE PROFILE

Biophysical Chemistry 202 (2015) 13–20

Contents lists available at ScienceDirect

Biophysical Chemistry

journal homepage: http://www.elsevier.com/locate/biophyschem

Interactions of the antiviral and antiparkinson agent amantadine with lipid membranes and human erythrocytes

Mario Suwalsky [a,*], Malgorzata Jemiola-Rzeminska [b,c], Mariella Altamirano [d], Fernando Villena [d], Nathan Dukes [e], Kazimierz Strzalka [b,c]

[a] Faculty of Chemical Sciences, University of Concepción, Concepción, Chile
[b] Faculty of Biochemistry, Biophysics and Biotechnology, Jagiellonian University, Krakow, Poland
[c] Malopolska Centre of Biotechnology, Jagiellonian University, Krakow, Poland
[d] Faculty of Biological Sciences, University of Concepción, Concepción, Chile
[e] Faculty of Medicine, P. Catholic University of Chile, Santiago, Chile

HIGHLIGHTS

- Interactions of amantadine with human erythrocytes and lipid bilayers were assessed.
- Amantadine changed the morphology of erythrocytes inducing formation of echinocytes.
- This change of shape indicates that it was inserted in the outer leaflet of the erythrocyte membrane.
- Amantadine interacted with a class of phospholipid present in the outer leaflet of the erythrocyte membrane.

GRAPHICAL ABSTRACT

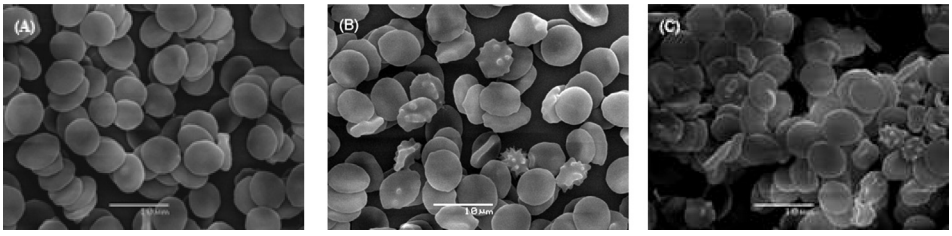

ARTICLE INFO

Article history:
Received 27 March 2015
Received in revised form 1 April 2015
Accepted 1 April 2015
Available online 9 April 2015

Keywords:
Amantadine
Erythrocyte membrane
Phospholipid bilayer

ABSTRACT

Aimed to better understand the molecular mechanisms of its interactions with cell membranes, human erythrocyte and molecular models of the red cell membrane were utilized. The latter consisted of bilayers of dimyristoylphosphatidylcholine (DMPC) and dimyristoylphosphatidylethanolamine (DMPE), representative of phospholipid classes located in the outer and inner monolayers of the human erythrocyte membrane, respectively. The capacity of amantadine to perturb the bilayer structures of DMPC and DMPE was evaluated by X-ray diffraction, fluorescence spectroscopy and differential scanning calorimetry (DSC). In an attempt to further elucidate its effects on cell membranes, the present work also examined amantadine influence on the morphology of intact human erythrocytes by means of scanning electron microscopy (SEM). Results indicated that amantadine induced morphological changes to human erythrocytes and interacted in a concentration-dependent manner with DMPC bilayers in contrast to DMPE that was hardly affected by the presence of the drug.

Abbreviations: RBCS, red blood cell suspension; SEM, scanning electron microscopy; DMPC, dimyristoylphosphatidylcholine; DMPE, dimyristoylphosphatidylcholine; DSC, differential scanning calorimetry; MLV, multilamellar vesicles.

* Corresponding author.
E-mail address: msuwalsk@udec.cl (M. Suwalsky).

http://dx.doi.org/10.1016/j.bpc.2015.04.002
0301-4622/

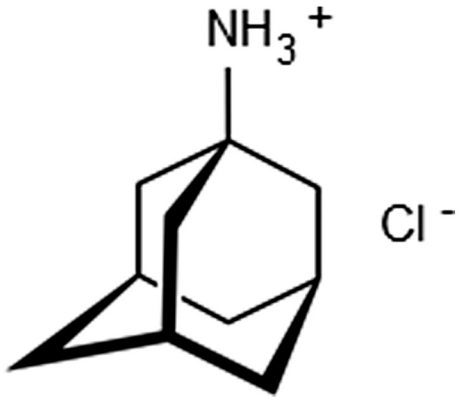

Fig. 1. Schematic formula of amantadine hydrochloride.

1. Introduction

Amantadine (1-aminoadamantane, Fig. 1), a glutaminergic receptor antagonist, is a stable quasi-spherical cyclic primary amine which is therapeutically used for both influenza and Parkinson's disease [1–5]. This compound inhibits viral replication by blocking the channel activity of the M2 proton channel that is critical in the virus life cycle [6]. It has been suggested that the mechanism of M2 channel inhibition would be due to amantadine interaction with the membrane side of the channel [7]. Association between amantadine and cellular membrane was first reported by Epand et al. [8] who demonstrated that the drug inhibited membrane fusion. Studies performed by neutron and X-ray diffraction on dioleoylphosphatidylcholine (DOPC) showed that the hydrophobic cyclic region of amantadine hydrochloride located between the phosphate and ester linkages of DOPC with the polar $^{+}NH_3$ group protruding into the water space [1]. A solution NMR study on dimyristoylphosphatidylcholine (DMPC) agreed in that amantadine localized near the negatively charged phosphate group and the hydrocarbon chain of DMPC [7]. A more recent work on solid-state NMR and molecular dynamics simulations reported that the long axis of amantadine located parallel to DMPC bilayer normal and its amino group was oriented toward the lipid head group [9].

Studies on the effects of amantadine on human erythrocytes are very scarce. It has been reported that side effects of amantadine treatment include anemia which could result from suicidal erythrocyte death or eryptosis, which accelerates the clearance of circulating erythrocytes [4]. Typical eryptosis is characterized by cell shrinkage and cell membrane scrambling. However, amantadine does not decrease cell volume; on the contrary, it produces cell swelling, effect that could not be satisfactorily explained [4]. Amantadine has also been shown to affect erythrocyte shape, inducing stomatocytosis [10]. With the aim to better understand the molecular mechanisms of the interaction of amantadine with cell membranes we have utilized human erythrocytes and molecular models of its membrane. Human erythrocytes were chosen because of their only single membrane and no internal organelles constitute an ideal cell system for studying interactions of chemical compounds with cell membranes [11]. On the other hand, although less specialized than many other cell membranes they carry on enough functions in common with them such as active and passive transport, and the production of ionic and electric gradients to be considered representative of the plasma membrane in general. The molecular models of the erythrocyte membrane consisted in bilayers of dimyristoylphosphatidylcholine (DMPC) and dimyristoylphosphatidylethanolamine (DMPE), representative of phospholipid classes located in the outer and inner monolayers of cell membranes, particularly of the human erythrocyte, respectively [12,13]. The capacity of amantadine to interact with the bilayer structures of DMPC and DMPE was evaluated by X-ray diffraction and differential scanning calorimetry (DSC), and of DMPC by fluorescence spectroscopy; intact human erythrocytes were observed by scanning electron microscopy (SEM). These systems and techniques have been used in our laboratories to determine the interaction with and the membrane-perturbing effects of other therapeutic compounds, including antiarrhythmic drugs [14–17].

2. Materials and methods

2.1. X-ray diffraction studies of DMPC and DMPE multilayers

The capacity of amantadine to interact with DMPC and DMPE multilayers was evaluated by X-ray diffraction. Synthetic DMPC (lot 140PC-24, MW 677.9) and DMPE (lot 140PE-54, MW 635.9) from Avanti Polar Lipids (AL, USA), and amantadine hydrochloride (MW 394.5) from Sigma-Aldrich (Milwaukee, USA) were used without further purification. About 2 mg of each phospholipid was introduced into Eppendorf tubes which were then filled with 200 l of (a) distilled water (control), and (b) aqueous solutions of amantadine in a range of concentrations (50 μM–100 μM for DMPC and 1 mM–10 mM for DMPE experiments). The specimens were shaken, incubated for 30 min at 30 °C and 60 °C with DMPC and DMPE, respectively and centrifuged for 10 min at 2400 rpm. Samples were then transferred into 1.5 mm diameter special glass capillaries (Glas-Technik&Konstruktion, Berlin, Germany) and X-ray diffracted utilizing Ni-filtered CuKα radiation from a Bruker Kristalloflex 760 (Karlsruhe, Germany) X-ray system. Specimen-to-film distances were 8 and 14 cm, standardized by sprinkling calcite powder on the capillary surface. The relative reflection intensities and interplanar spacings were obtained from an MBraun PSD-50 M linear position-sensitive detector system (Garching, Germany) and ASA software; no correction factors were applied. Data analyses were performed by means of Origin 3.0 software (Origin Lab Corp., USA). The experiments were performed at 19 °C and 1 °C, which is below the main phase transition temperature of both DMPC and DMPE. Higher temperatures would have induced transitions onto fluid phases making the detection of structural changes harder. Each experiment was performed in triplicate.

2.2. Differential scanning calorimetry (DSC) studies on DMPC and DMPE liposomes

Appropriate amounts of DMPC or DMPE dissolved in chloroform were gently evaporated to dryness under a stream of gaseous nitrogen until a thin film on the wall of the glass test tube was formed. To remove the remnants of moisture, the samples were subsequently exposed to vacuum for 1 h and then dry lipid films were suspended in distilled water. Amantadine was added in the concentration range of 0.10 to 10 mM for DMPC and 0.10 to 1.0 mM for DMPE. The multilamellar liposomes (MLV) were prepared by vortexing the samples at the temperature above gel-to-liquid crystalline phase transition of the pure lipid (about 30 °C for DMPC and 60 °C for DMPE). DSC experiments were performed using a NANO DSC Series III System with Platinum Capillary Cell (TA Instruments, USA). The calorimeter was equipped with the original data acquisition and analysis software. In order to avoid bubble formation during heating mode the samples were degassed prior to being loaded by pulling a vacuum of 0.3–0.5 atm on the solution for a period of 10–15 min. Then the sample cell was filled with about 400 μl of MLV suspension and an equal volume of buffer was used as a reference. The cells were sealed and thermally equilibrated for about 10 min below starting temperature of the run. All measurements were made on samples under 3-bar pressure. The data were collected in the range of 0–40 °C (DMPC) and 30–70 °C (DMPE) at the scan rate 1 °C min^{-1} both for heating and cooling. Scans of buffer as a sample and a reference were also performed to collect the apparatus baseline. In order to check the reproducibility, each sample was prepared and recorded at least three times. Each data set was analyzed for thermodynamic parameters with the software package supplied by TA Instruments.

2.3. Fluorescence measurements of large unilamellar vesicles (LUV) and of isolated unsealed human erythrocyte membranes (IUM)

The influence of amantadine on the physical properties of DMPC LUV and IUM was examined by fluorescence spectroscopy using DPH and laurdan (Molecular Probe, Eugene, OR, USA) fluorescent probes. DPH is widely used as a probe for the hydrophobic regions of the phospholipid bilayers because of its favorable spectral properties. Their steady-state fluorescence anisotropy measurements were used to investigate the structural properties of DMPC LUV and IUM as it provides a measure of the rotational diffusion of the fluorophor restricted within a certain region such as a cone due to the lipid acyl chain packing order. Laurdan, an amphiphilic probe, has high excitation sensitivity and emission spectra to the physical state of membranes. With the fluorescent moiety within a shallow position in the bilayer, laurdan provides information about the polarity and/or molecular dynamics at the level of the phospholipid glycerol backbone. The quantification of the laurdan fluorescence spectral shift was effected by means of the general polarization (GP) concept [18]. DMPC LUV suspended in water were prepared by extrusion of frozen and thawed multilamellar liposome suspensions (final lipid concentration 0.4 mM) through two stacked polycarbonate filters of 400 nm pore size (Nucleopore, Corning Costar Corp., MA, USA) under nitrogen pressure at 10 °C above the lipid phase transition temperature. Erythrocytes were separated from heparinized venous blood samples obtained from normal casual donors by centrifugation and washing procedures. IUM were prepared by lysis, according to Dodge et al. [19]. DPH and laurdan were incorporated into LUV and IUM by addition of 2 μl/ml aliquots of 0.5 mM solutions of the probe in dimethylformamide and ethanol, respectively, in order to obtain final analytical concentrations of 1×10^{-3} mM, and incubated them at 37 °C for 45 min. Fluorescence spectra and anisotropy measurements were performed in a phase shift and modulation K_2 steady-state and time resolved spectrofluorometer (ISS, Inc., Champaign, IL, USA) interfaced to computer. Software from ISS was used for both data collection and analysis. LUV suspension measurements were carried out at 18 °C and 37 °C, and IUM measurements were made at 37 °C using 10 mm path-length square quartz cuvettes. Sample temperature was controlled by an external bath circulator (Cole-Parmer, Chicago, IL, USA) and monitored before and after each measurement using an Omega digital thermometer (Omega Engineering Inc., Stanford, CT, USA). Anisotropy measurements were made in the L configuration using Glan Thompson prism polarizers (I.S.S., Inc.) in both exciting and emitting beams. The emission was measured by means of a WG-420 Schott high-pass filter (Schott WG-420, Mainz, Germany) with negligible fluorescence. DPH fluorescence anisotropy (r) was calculated according to the definition: $r = (I_{\parallel} - I_{\perp}) / (I_{\parallel} + 2I_{\perp})$, where $I_{\parallel}$ and $I_{\perp}$ are the corresponding parallel and perpendicular emission fluorescence intensities with respect to the vertically polarized excitation light [20]. Laurdan fluorescence spectral shifts were quantitatively evaluated using the GP concept (see above) which is defined by the expression $GP = (I_b - I_r) / (I_b + I_r)$, where I_b and I_r are the emission intensities at the blue and red edges of the emission spectrum, respectively. These intensities have been measured at the emission wavelengths of 440 and 490 nm, which correspond to the emission maxima of laurdan in both gel and liquid crystalline phases, respectively [21]. Amantadine was incorporated into LUV and IUM suspensions by addition of adequate (10 mM) aliquots of concentrated solutions in order to obtain the different concentrations used in this work. Samples thus prepared were then incubated at 37 °C, for ca. 15 min and measured at 18 °C and 37 °C; at 18 °C because the X-ray experiments were performed at about this temperature, and at 37 °C because that is the normal temperature at which erythrocytes circulate in humans. Blank subtraction was performed in all measurements using unlabeled samples without probes. Data presented in Fig. 6 represent mean values and standard error of ten measurements in two independent samples. Unpaired Student's *t*-test was used for statistical calculations.

2.4. Scanning electron microscopy (SEM) studies on human erythrocytes

One blood drop from a human healthy donor not receiving any pharmacological treatment was obtained by puncturing a previously disinfected ear and received in an Eppendorff tube containing 100 μl of heparin (5000 UI/ml) in 900 μl of phosphate buffer saline (PBS), pH 7.4. Red blood cells were centrifuged (1000 rpm × 10 min), washed three times in PBS and bovine serum albumin (BSA) and then distributed in several Eppendorf tubes that were centrifuged; the supernatants were replaced by 100 μl of amantadine in a range of concentrations, and then incubated at 37 °C for 1 h, period in line with the larger effects induced by compounds on red cell shape [22,23]. Controls were cells resuspended PBS without amantadine. Samples were incubated at 37 °C for 1 h and centrifuged at 1000 rpm for 10 min, the supernatant was replaced by 1000 μl of 2.5% glutaraldehyde and left to rest for 24 h at 5 °C. Samples were washed three times in distilled water and centrifuged (1000 rpm × 10 min.); about 20 μl of each sample was placed on siliconized Al glass covered stubs, air-dried at room temperature, gold coated for 3 min at 13.3 Pa in a sputter device (Edwards S 150, Sussex, England), and examined in a scanning electron microscope (JEOL JSM-6380LV, Japan).

3. Results

3.1. X-ray diffraction studies of DMPC and DMPE multilayers

Fig. 2A exhibits results obtained by incubating DMPC with water and amantadine. As expected, water altered the structure of DMPC as its bilayer repeat (phospholipid bilayer width plus the layer of water) increased from about 55 Å in its dry crystalline form to 64.5 Å when immersed in water, and its small-angle reflections, which correspond to DMPC polar terminal groups, were reduced to only the first two orders of the bilayer width. On the other hand, only one strong reflection of 4.2 Å showed up in the wide-angle region which corresponds to the average distance between fully extended acyl chains organized with rotational disorder in hexagonal packing [24]. These results were indicative of the less ordered state reached by DMPC bilayers. Fig. 2A discloses that after being exposed to 60 μM amantadine concentration there was a considerable weakening of the small- and wide-angle reflection intensities (indicated as SA and WA in the figure, respectively)

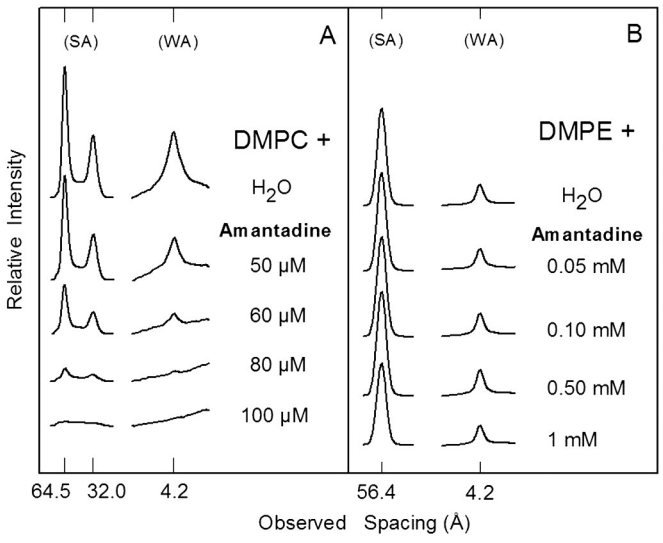

Fig. 2. Microdensitograms from X-ray diffraction patterns of DMPC (A) and DMPE (B) in water and aqueous solutions of amantadine hydrochloride; (SA) small-angle and (WA) wide-angle reflections.

which with 100 μM concentration practically disappeared. From these results it can be concluded that amantadine produced a significant structural perturbation of DMPC bilayers. Fig. 2B shows the results of the X-ray diffraction analysis of DMPE bilayers incubated with water and amantadine. As reported elsewhere, water did not significantly affect the bilayer structure of DMPE [24]. Fig. 2B shows that increasing concentrations of amantadine did not cause any significant effect on DMPE reflection intensities, all of which still remained practically unchanged even with 1 mM amantadine.

3.2. Differential scanning calorimetry (DSC) studies on DMPC and DMPE liposomes

Fully hydrated DMPC and DMPE bilayers in the absence of any additives, showed a well-defined and known thermal behavior. In the temperature range of 0–30 °C DMPC liposomes exhibited a strong and sharp main transition at 23.83 °C, with an enthalpy change (ΔH) of 21.46 kJ mol^{-1} which arises from the conversion of the rippled gel phase ($P_{\beta'}$) to the lamellar liquid-crystal (L_α) phase. Here, the transition temperature corresponds to the transition peak at the maximal peak heat and the transition enthalpy is equal to the integrated area under the peak divided by the lipid concentration. The transition was reversible and hysteresis of about 0.77 °C was observed between the heating and cooling processes ascribed to the formation of an intermediate metastable phase that slowly interconverts to the L_α phase [25]. The shape of the peak was roughly symmetrical, with only a slight skewing toward lower temperatures. At 14.71 °C, a pretransition arising from the conversion of a lamellar gel phase (L_β) to a rippled gel phase was observed, with ΔH of 2.93 kJ mol^{-1}. DMPE liposomes exhibited a single sharp transition at 50.60 °C; with an enthalpy change of 28.15 kJ mol^{-1}in the 30–70 °C thermal range. This transition, designated as transformation of the gel phase (L_β) to the L_α phase, was highly reproducible, strong and sharp, with a nearly symmetrical profile. The thermodynamic data of the pure DMPC and DMPE are consistent with previous reports [26–28].

In Fig. 3A, a set of the representative high-sensitivity DSC heating thermograms is depicted that were obtained for pure DMPC multibilayer vesicles and binary mixtures of DMPC and amantadine at 0.1 to 10 mM content. Upon the addition of the drug, thermotropic phase behavior of DMPC changed and as a result it was observed a gradual diminishing of the main phase transition peak and its shift to the lower temperatures. Moreover, amantadine affected the pretransition of DMPC bilayer; however, it was still retained at as high drug concentration as 10 mM. Illustrated in Fig. 3B, heating profiles recorded for DMPE bilayers showed considerably smaller ability of amantadine to distort the phase transition of the phospholipid molecules bearing ethanolamine moiety. The effectiveness in perturbations of DMPE thermotropic phase transition exerted by amantadine was further analyzed in terms of thermodynamic parameters. Tables 1 and 2 present values of temperature, enthalpy and entropy for DMPC and DMPE systems, respectively, determined on the basis of heating and cooling scans. In Fig. 4 the values of the main-transition (T_m) and pretransition (T_p) temperatures are plotted as a function of the amantadine concentration. As a general feature, both in heating and cooling processes in the presence of amantadine a non-linear decrease of T_m and T_p was observed. Additionally, from Fig. 4A it could be seen that for DMPC bilayers pretransition was abolished during cooling at drug concentrations higher than 0.5 mM. While the presence of amantadine in DMPC bilayer at the concentration range up to 10 mM resulted in gradual decrease of T_m, Fig. 4B shows that T_m of DMPE membrane decreases up to 0.5 mM and remains constant thereafter, especially during cooling. Lowering of DMPC main phase transition and DMPE transition in concentration-dependent manner is presented in Fig. 5. When present at 1 mM, amantadine caused a decline of transition peak height by 38% and 29% in case of DMPC and DMPE bilayers, respectively.

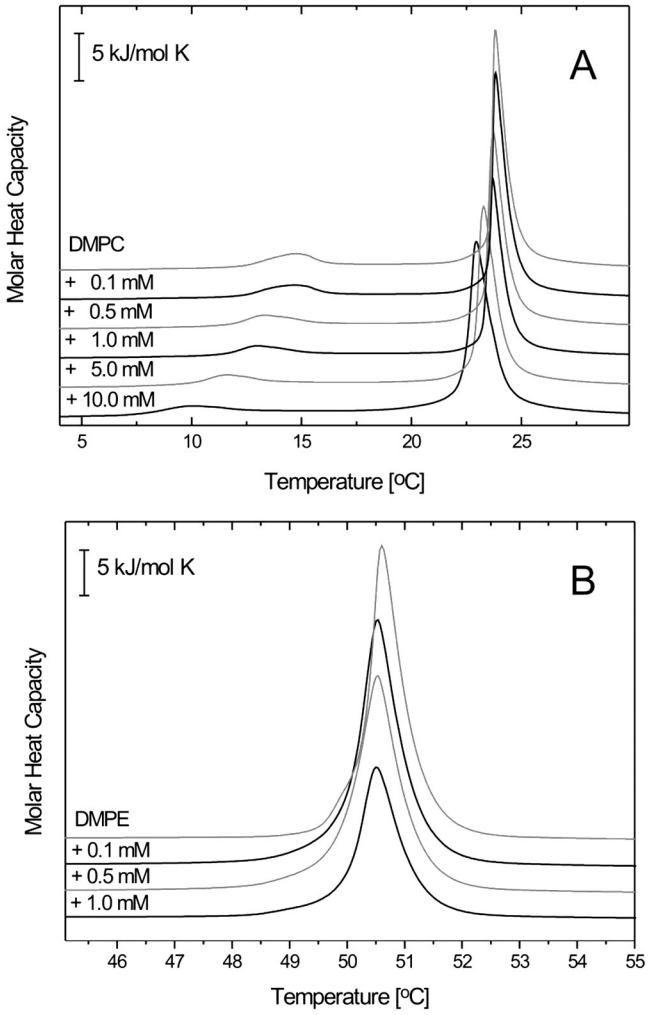

Fig. 3. Representative DSC curves obtained for multilamellar DMPC (A) and DMPE (B) liposomes containing amantadine hydrochloride at various concentrations. Scans were obtained at a heating rate of 1 °C min^{-1}.

3.3. Fluorescence measurements of large unilamellar vesicles (LUV) and of isolated unsealed human erythrocyte membranes (IUM)

The concentration-dependent effects of amantadine on DMPC LUV and IUM were explored at two different depths of their bilayers: at the deep hydrophobic core determined by DPH steady-state fluorescence anisotropy (r), and at the hydrophilic/hydrophobic level, estimated from laurdan fluorescence spectral shift through the GP parameter. These effects were studied at 18 °C and 37 °C on DMPC LUV and at 37 °C on IUM. The steady state fluorescence anisotropy of DPH as a function of the additive in DMPC LUV is depicted in Fig. 6A. A very sharp decrease was observed in the bilayer gel state (18 °C) at 10 μM amantadine, result that can be interpreted as an acute structural disordering of DMPC acyl chains. However, the opposite effect was produced at 37 °C when the bilayer was in a fluid liquid crystalline phase. As shown in Fig. 6B, 10 μM amantadine sharply increased laurdan GP at 18 °C, effect that can be interpreted as an acute structural ordering of the polar head group region of DMPC bilayer; however, at 37 °C once again the opposite effect was induced. From these results it can be concluded that amantadine interacted with both DMPC regions producing opposite effects: in its gel phase (18 °C) ordering its polar head groups and disordering the hydrophobic acyl chains whereas in the liquid crystalline phase (37 °C) ordered the polar groups and disordered the acyl chains. Fig. 6C presents the results observed

Table 1
Thermodynamic parameters of the pretransition and main phase transition of pure, fully hydrated DMPC multilamellar liposomes and DMPC/amantadine mixtures determined from heating and cooling scans collected at a heating (cooling) rate of 1 °C min^{-1}. The accuracy for the main phase transition temperature and enthalpy was ±0.01 °C and ±0.8 kJ/mol, respectively.

Compound	Pretransition heating			Main transition heating			Pretransition cooling			Main transition cooling		
Conc [mM]	ΔH [kJ/mol]	ΔS [J/molK]	T_p [°C]	ΔH [kJ/mol]	ΔS [J/molK]	T_m [°C]	ΔH [kJ/molK]	ΔS [J/molK]	T_p [°C]	ΔH [kJ/mol]	ΔS [J/molK]	T_m [°C]
DMPC												
1.0	2.93	1.02	14.71	21.46	7.23	23.83	1.30	0.46	9.04	20.34	6.87	23.06
+ amantadine												
0.1	2.76	0.96	14.64	21.25	7.11	23.83	1.29	0.46	9.00	17.45	5.89	23.06
0.5	2.75	0.96	13.30	20.71	6.97	23.73	1.10	0.42	8.56	18.50	6.25	22.93
1.0	2.17	0.76	12.96	18.93	6.28	23.66	–	–	–	16.07	5.43	22.82
5.0	1.85	0.65	11.59	21.41	7.22	23.28	–	–	–	18.45	6.24	22.41
10.0	1.53	0.54	9.94	25.87	8.74	22.94	–	–	–	22.01	7.46	22.03

from the interaction of amantadine with erythrocyte membranes at 37 °C. A significant decrease was observed in laurdan GP in the drug 10–100 μM range concentration; on the other hand, 10 μM amantadine produced a sharp increase in DPH anisotropy and then a sharp decrease; these results imply that amantadine mostly perturbed the hydrophobic core of the erythrocyte membrane bilayer. It is worthwhile to be mentioned that most of these effects were produced with the lowest assayed amantadine concentrations (10 μM).

3.4. Scanning electron microscopy (SEM) studies of human erythrocytes

The effects of the interaction of amantadine with human erythrocytes were evaluated *in vitro* by SEM. The resulting micrographs (Fig. 7) show that the drug induced notorious changes in the morphology of the red blood cells. The normal resting shape of the human red blood cell is a flat biconcave disc (discocyte) ~8 μm diameter which can be observed in Fig. 7A, corresponding to the erythrocytes incubated with PBS 1× (pH 7.4) (control). On the other hand, morphological analysis of the results revealed that amantadine changed the normal shape of the red blood cells in a dose-dependent manner. Fig. 7B (50 μM) clearly shows that discocytes underwent a partial transformation into echinocytes (erythrocytes with crenated shapes), and 100 μM amantadine (Fig. 7C) somewhat increased the number of echinocytes.

4. Discussion

Interactions with biological membranes are of utmost importance for drug's pharmacokinetic (molecular pathway to specific receptor site) and pharmacodynamic (specific interactions with high affinity receptor sites) actions. It is not only dependent on their partitioning into lipid bilayer and drug permeability but also their therapeutic target are often anchored in membranes. Moreover, it is believed that numerous cardiovascular and other diseases are related to modifications of membrane lipid composition and structure. Our studies here represent an attempt to analyze the molecular basis of membrane structural perturbations induced by amantadine using the human erythrocyte membrane as a model membrane system. In order to understand the location and interaction of amantadine with the erythrocyte membrane lipid bilayer, molecular models constituted by DMPC and DMPE bilayers were used. These are classes of lipids preferentially located in the outer and inner monolayers of the human erythrocyte membrane, respectively [12,13]. Results by X-ray diffraction on the interaction of amantadine with DMPC showed that the drug produced a significant structural perturbation of the lipid bilayer whereas no effects were observed in DMPE, even at ten times higher drug concentrations (Fig. 2). DMPC and DMPE differ only in their terminal amino groups, these being $^{+}N(CH_3)_3$ in DMPC and $^{+}NH_3$ in DMPE. DMPE molecules pack tighter than those of DMPC due to their smaller polar groups and higher effective charge,

Table 2
Thermodynamic parameters of the phase transition of pure, fully hydrated DMPE multilamellar liposomes and DMPE/amantadine mixtures determined from heating and cooling scans collected at a heating (cooling) rate of 1 °C min^{-1}. The accuracy for the main phase transition temperature and enthalpy was ±0.01 °C and ±0.8 kJ/mol, respectively.

Compound		Heating			Cooling		
	Conc [mM]	ΔH [kJ/mol]	ΔS [J/molK]	T_m [°C]	ΔH [kJ/mol]	ΔS [J/molK]	T_m [°C]
DMPE							
	1.00	28.15	8.70	50.60	22.35	6.93	49.33
+ amantadine							
	0.10	27.94	8.63	50.54	28.40	8.82	48.95
	0.50	26.44	8.17	50.54	25.71	7.99	48.81
	1.00	17.61	5.44	50.50	15.09	4.69	48.80

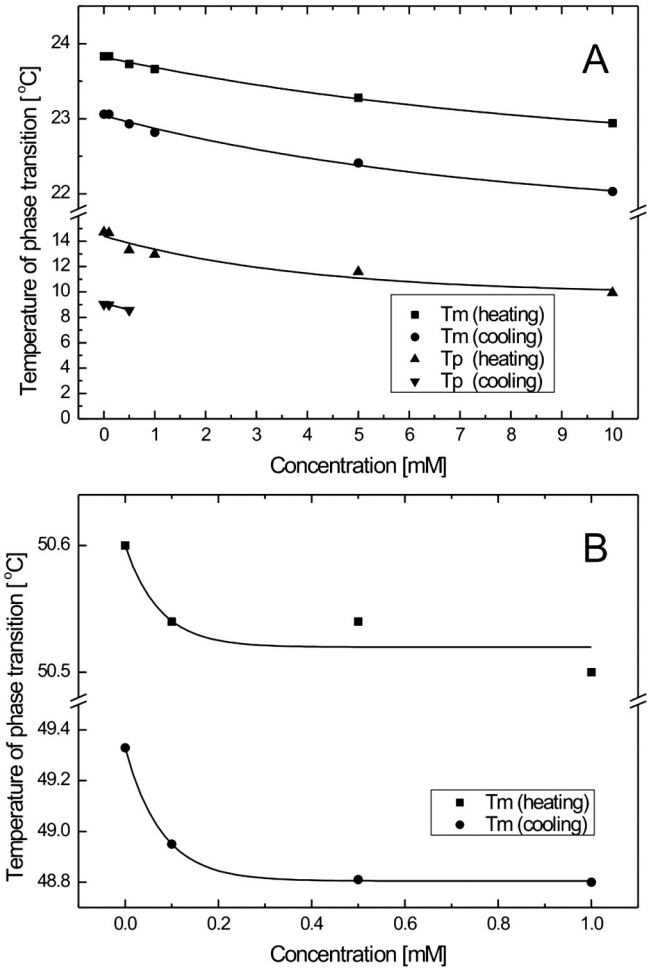

Fig. 4. A plot of phase transition temperature of DMPC (A) and DMPE (B) multilamellar liposomes determined for cooling and heating scans as a function of amantadine hydrochloride content.

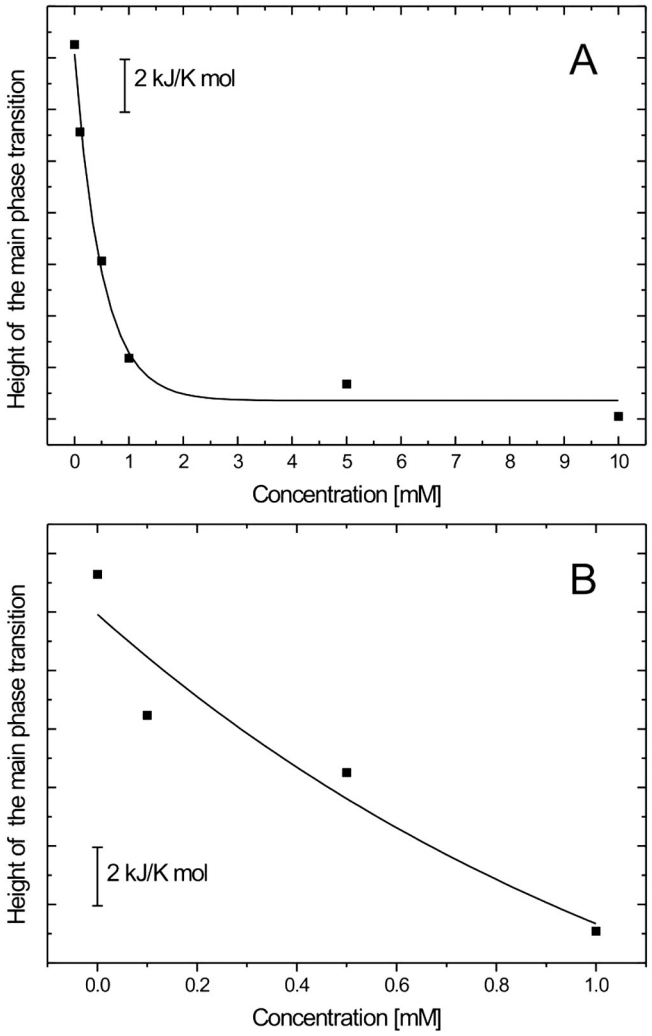

Fig. 5. A plot of height of DMPC main phase transition (A) and DMPE phase transition (B) determined on the basis of heating scans as a function of amantadine hydrochloride content.

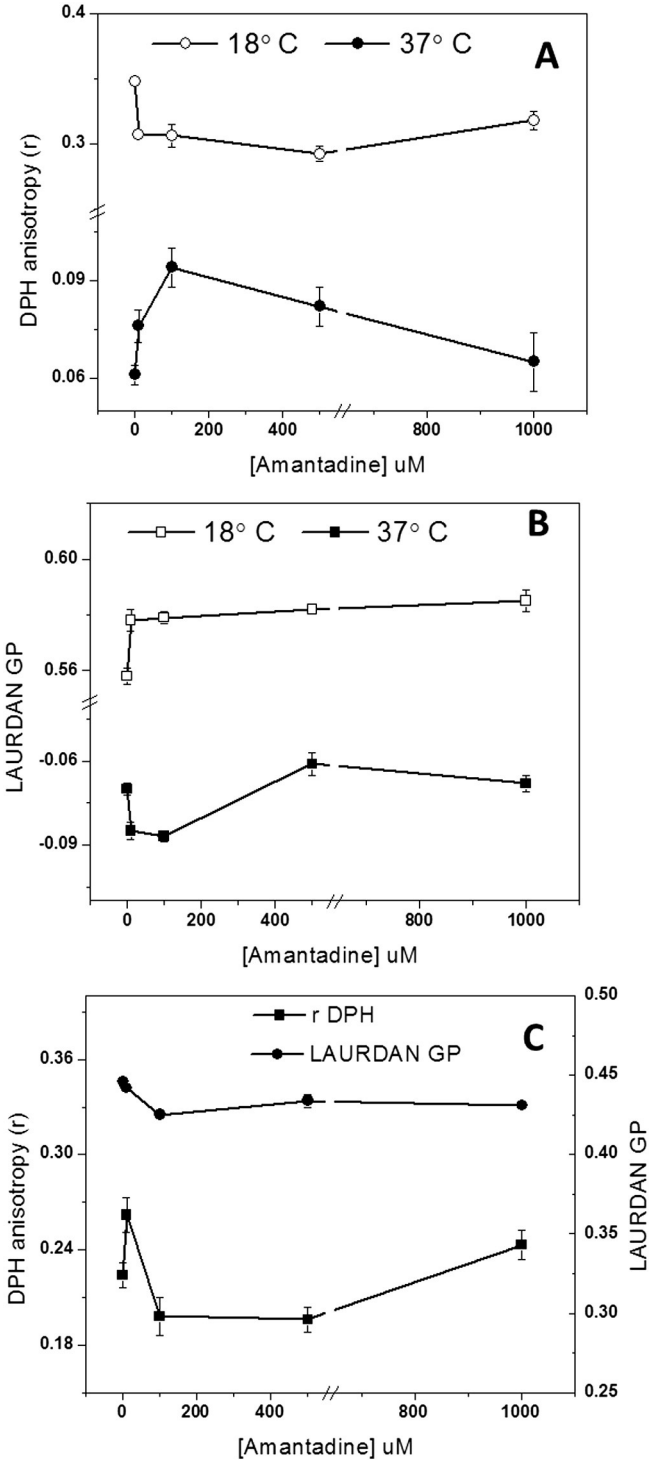

Fig. 6. Effect of amantadine hydrochloride on (A) the fluorescence anisotropy (r) of DPH, on (B) the generalized polarization (GP) of laurdan in DMPC LUV at 18 °C and 37 °C, and on (C) IUM at 37 °C. Each point represents an average of data in duplicate and standard error.

resulting in a very stable bilayer system held by electrostatic interactions and hydrogen bonds. However, the hydration of DMPC results in water filling the highly polar interbilayer spaces with the resulting increase of their width [24]. This phenomenon might allow the incorporation of the positively charged amantadine molecules into DMPC bilayers and their consequent interaction. In fact, it was observed that amantadine in a concentration as low as 60 μM induced a considerable weakening of the small- and wide-angle reflection intensities (indicated as SA and WA in the figure, respectively) which with a 100 μM concentration all reflections practically disappeared. This result implies that both the polar and hydrophobic regions of DMPC were perturbed by the insertion of the drug in the lipid bilayer. It is very likely that the tricyclodecane moiety is in contact with the lipid alkyl chains, while a positively charged amine group of amantadine interacts with the negatively charged phosphate of the lipid headgroup; the latter interactions would lead to a disruption of the electrostatic attractions and hydrogen bonds that maintain DMPC molecules in their bilayer arrangement.

Previous studies on the interaction of amantadine with lipid bilayers have generated confusing conclusions about the location of amantadine within the lipid bilayer [9]. Neutron and X-ray diffraction experiments performed on multilayers of dioleoylphosphatidylcholine (DOPC) concluded that the uncharged amantadine had two populations, one that was nearly at the bilayer center and one at the water/bilayer interface [1]. Another study, carried out by EPR on DMPC, dipalmitoylphosphatidylcholine (DPPC) and distearoylphosphatidylcholine (DSPC) liposomes concluded that amantadine could penetrate into the gel-phase membrane practically with the same partitioning as into the fluid-phase membrane, and that in both cases a significant part of amantadine was located deep in the acyl chain region of the lipid bilayer [2]. A molecular-dynamics simulation on the location of amantadine in palmitoyloleoylphosphatidylcholine (POPC) concluded that the drug formed substantial interactions with the lipid head group, and its orientation is such that the tricyclodecane moiety is in contact with the lipid acyl

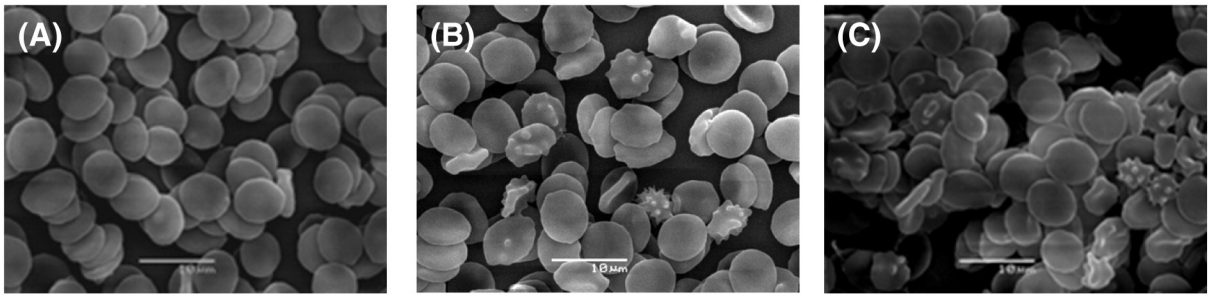

Fig. 7. Effect of amantadine on the morphology of human erythrocytes. Images obtained by scanning electron microscopy (SEM) of (A) control, (B) incubated with 50 μM, and (C) with 100 μM amantadine hydrochloride.

chains, and the ammonium group is in contact with the lipid head group, in particular the glycerol oxygens [3]. Our X-ray diffraction results tend to agree with the conclusion reached by Chew et al. [3]. However, we believe that phosphate instead of glycerol oxygens interact with the amantadine charged amine group; as explained above, this interaction would be responsible for the structural perturbation induced by the drug to DMPC polar region. Moreover, our fluorescence spectroscopy results coincided in that amantadine located in both the polar head and acyl chain regions of DMPC in both the gel and liquid crystalline phases.

To the best of our knowledge, little is reported about thermotropic behavior of membrane models in the presence of adamantanes, and even more so there are no DSC studies on the influence of amantadine on phospholipids. Calorimetric measurements performed on DMPC liposomes showed that amantadine was capable of distortion of both pretransition and main phase transition of lipids that form a bilayer. As a small molecule, with its experimentally determined log P value of 2.44 [29], amantadine is a very lipophilic compound and could penetrate easily into the core of the lipid bilayer. This leads to reduction of interfacial tension and affects the lateral interaction between the apolar fatty acid chains. The presence of the polar head group on the phospholipids gives rise to specific and direct interactions between DMPC molecules and amine group of a drug. As a result, we observed the decrease of molar heat capacity and broadening of the main phase transition as well as its shift to the lower values. Significantly, smaller effect of amantadine on DMPE liposomes shown in the calorimetric studies was probably related to the tight packing of this lipid, whose head group occupies a molar area smaller by about 8 $Å^2$ in comparison with that of DMPC [30]. Being distributed within DMPC bilayer homogenously, amantadine molecules despite small size and lipophilic properties were unable to penetrate the hydrophobic core of DMPE. It can then be assumed that smaller miscibility of amantadine with DMPE liposomes may arise from the fact that van der Waals interactions between the lipid acyl chains themselves are much stronger than those in which amantadine molecules participate.

SEM *in vitro* observations showed that amantadine induced morphological alterations to human red cells from their normal discoid shape to echinocytes. According to the bilayer couple hypothesis [31, 32] shape changes induced in erythrocytes by foreign molecules are due to differential expansion of the two monolayers of the red cell membrane. Thus, cup-shaped stomatocytes are formed when the compound inserts into the inner monolayer whereas spiculated-shaped echinocytes are produced when it locates into the outer moiety. The finding that amantadine induced the formation of echinocytes indicates that it was inserted in the outer leaflet of the erythrocyte membrane. This conclusion is supported by X-ray and calorimetric experiments carried out in DMPC and DMPE bilayers, In fact, results showed that amantadine mostly interacted with DMPC, which is preferentially located in the outer monolayer of the human erythrocyte membrane. There are very scanty reports related to morphological changes induced by amantadine to human erythrocytes. In one of them, Tverdislov et al. [10] found that amantadine induced the formation of stomatocytes. The difference with our results might be due to the higher drug concentration they used (2.66 mM and 5.32 mM). In general, plasma amantadine levels range from about 7 μM after therapeutic doses [33], about 16 μM in patients with toxic symptoms, and up to about 0.13 mM in lethal concentration [34]. It is important to emphasize that the effects of amantadine detected in the present work, particularly at the erythrocyte membrane level, were observed at a concentration range of 10–50 μM, which is somewhat higher than the plasma therapeutic concentration. However, it must be taken into account that these were biophysical studies *in vitro* carried out, which usually require high concentrations in order to detect drug effects.

In conclusion, our experimental findings are certainly of interest as they have demonstrated that amantadine interacts with the human erythrocyte membrane affecting the cell morphology. It must be considered that alteration of the normal biconcave shape of red blood cells increases their resistance to entry into capillaries, which could contribute to a decreased blood flow, loss of oxygen, and tissue damage through microvascular occlusion [35,36]. Functions of ion channels, receptors and enzymes immersed in cell membrane lipid moieties also might be affected.

Acknowledgments

To C.P. Sotomayor, L.F. Aguilar and F. Neira for technical assistance. This work was supported by FONDECYT (project 1130043). Calorimetric measurements were carried out using the instrument purchased thanks to financial support of European Regional Development Fund (contract no. POIG.02.01.00-12-167/08, project Malopolska Centre of Biotechnology).

References

[1] K.C. Duff, A.J. Cudmore, J.P. Bradshaw, The location of amantadine hydrochloride and free base within phospholipid mltilayers: a neutron and X-ray diffraction study, Biochim. Biophys. Acta 1145 (1993) 149–156.
[2] W.K. Subczynski, J. Wojas, V. Pezeshk, A. Pezeshk, Partitioning and localization of spin-labeled amantadine in lipid bilayers: an EPR study, J. Pharm. Sci. 87 (1998) 1249–1254.
[3] C.F. Chew, A. Guy, P.C. Biggin, Distribution and dynamics of adamantanes in a lipid bilayer, Biophys. J. 95 (2008) 5627–5636.
[4] M. Föller, C. Geiger, H. Mahmud, J. Nicolay, F. Lang, Stimulation of suicidal erythrocyte death by amantadine, Eur. J. Pharmacol. 581 (2008) 13–18.
[5] N. Nishikawa, M. Nagai, T. Moritoyo, H. Yabe, M. Nomoto, Parkinsonism and related disorders, Parkinsonism Relat. Disord. 15 (2009) 351–353.
[6] L.H. Pino, L.J. Holsinger, R.A. Lamb, Influenza virus M2 protein has ion channel activity, Cell 69 (1992) 517–528.
[7] J. Wang, J.R. Schnell, J.J. Chou, Amantadine partition and localization in phospholipid membrane: a solution NMR study, Biochem. Biophys. Res. Commun. 324 (2004) 212–217.
[8] R.M. Epand, R.F. Epand, R.C. McKenzie, Effects of viral chemotherapeutic agents on membrane properties. Studies of cyclosporine A, benzyloxycarbonyl-D-Phe-L-Phe-Gly and amantadine, J. Biol. Chem. 262 (1987) 1526–1529.
[9] C. Li, M. Yi, J. Hu, H.-X. Zhou, T.A. Cross, Solid-state and MD simulations of the antiviral drug amantadine solubilized in DMPC bilayers, Biophys. J. 94 (2008) 1295–1302.
[10] V.A. Tverdislov, S. El-Karadagi, I.G. Kharitonenkov, R. Glaser, E. Donath, A. Herrmann, P. Lentzsch, J. Donath, Interaction of the antivirus agents remantadine and amantadine with lipid membranes and the influence on the curvature of human red cells, Gen. Physiol. Biophys. 5 (1986) 61–75.

[11] J.Y. Chen, W.H. Huestis, Role of membrane lipid distribution in chlorpromazine-induced shape change of human erythrocytes, Biochim. Biophys. Acta 1323 (1997) 299–309.
[12] J.M. Boon, B.D. Smith, Chemical control of phospholipid distribution across bilayer membranes, Med. Res. Rev. 22 (2000) 251–281.
[13] P.F. Devaux, A. Zachowsky, Maintenance and consequences of membrane phospholipids asymmetry, Chem. Phys. Lipids 73 (1994) 107–120.
[14] M. Suwalsky, I. Sánchez, M. Bagnara, C.P. Sotomayor, Interaction of antiarrhythmic drugs with model membranes, Biochim. Biophys. Acta 1195 (1994) 189–196.
[15] M. Suwalsky, J. Belmar, F. Villena, M.J. Gallardo, M. Jemiola-Rzeminska, K. Strzalka, Acetylsalicylic acid (aspirin) and salicylic acid interaction with the human erythrocyte membrane bilayer induce in vitro changes in the morphology of erythrocytes, Arch. Biochem. Biophys. 539 (2013) 9–19.
[16] M. Suwalsky, P. Zambrano, S. Mennickent, F. Villena, C. Sotomayor, L.F. Aguilar, S. Bolognin, Effects of phenylpropanolamine (PPA) on in vitro human erythrocyte membranes and molecular models, Biochem. Biophys. Res. Commun. 406 (2011) 320–325.
[17] M. Suwalsky, M. Manrique, F. Villena, C.P. Sotomayor, Structural effects in vitro of the anti-inflammatory drug diclofenac on human erythrocytes and molecular models of cell membranes, Biophys. Chem. 141 (2009) 34–40.
[18] T. Parasassi, E. Gratton, Membrane lipid domains and dynamics as detected by laurdan fluorescence, J Fluoresc. 5 (1995) 59–69.
[19] J.T. Dodge, C. Mitchell, C.D. Hanahan, The preparation and chemical characterization of haemoglobin-free ghosts of human erythrocytes, Arch. Biochem. Biophys. 100 (1963) 119–130.
[20] J.R. Lakowicz, Principles of Fluorescence Spectroscopy, Plenum, New York, 1999.
[21] T. Parasassi, G. De Stasio, A. D'Ubaldo, E. Gratton, Phase fluctuation in phospholipid membranes revealed by laurdan fluorescence, Biophys. J. 57 (1990) 1179–1186.
[22] B. Zimmermann, D.M. Soumpasis, Effects of monovalent cations on red cell shape and size, Cell Biophys. 7 (1985) 115–127.
[23] S.V.P. Malheiros, M.A. Brito, D. Brites, M.N. Correa, Membrane effects of trifluoperazine, dibucaine and praziquantel on human erythrocytes, Chem. Biol. Interact. 126 (2000) 79–95.
[24] M. Suwalsky, Phospholipid bilayers, in: J.C. Salamone (Ed.)Polymeric Materials Encyclopedia, vol. 7, CRC, Boca Raton, FL 1996, pp. 5073–5078.
[25] B. Tenchov, On the reversibility of the phase transitions in lipid–water systems, Chem. Phys. Lipids 57 (1991) 165–177.
[26] D. Marsh, General features of phospholipid phase transitions, Chem. Phys. Lipids 57 (1991) 109–120.
[27] R. Koynova, M. Caffrey, Phases and phase transitions of the phosphatidylcholines, Biochim. Biophys. Acta 1376 (1998) 91–145.
[28] R.N. Lewis, R.N. McElhaney, Calorimetric and spectroscopic studies of the polymorphic phase behavior of a homologous series of n-saturated 1,2-diacyl phosphatidylethanolamines, Biophys. J. 64 (1993) 1081–1096.
[29] http://www.drugbank.ca.
[30] A. Sujak, K. Strzalka, W.I. Gruszecki, Thermotropic phase behaviour of lipid bilayers containing carotenoid pigment canthaxanthin: a differential scanning calorimetry study, Chem. Phys. Lipids 145 (2007) 1–12.
[31] M.P. Sheetz, S.J. Singer, Biological membranes as bilayer couples. A molecular mechanism of drug-erythrocyte induced interactions, Proc. Natl. Acad. Sci. U. S. A. 71 (1974) 4457–4461.
[32] G. Lim, M. Wortis, Stomatocyte–discocyte–echinocyte sequence of the human red blood cell: evidence for the bilayer-couple hypothesis from membrane mechanics, Proc. Natl. Acad. Sci. U. S. A. 99 (2002) 16766–16769.
[33] F.G. Hayden, H.E. Hoffman, D.A. Spyker, Differences in side effects of amantadine hydrochloride and rimantadine hydrochloride relate to differences in pharmacokinetics, Antimicrob. Agents Chemother. 23 (1983) 458–464.
[34] R. Regenthal, M. Krueger, C. Koeppel, R. Preiss, Drug levels: therapeutic and toxic serum/plasma concentrations of common drugs, J. Clin. Monit. Comput. 15 (1999) 529–544.
[35] S.L. Winski, D.E. Carter, Arsenate toxicity in human erythrocytes: characterization of morphological changes and determination of the mechanism of damage, J. Toxicol. Environ. Health A 53 (1998) 345–355.
[36] S. Svetina, D. Kuzman, R.E. Waugh, P. Zibert, B. Zeks, The cooperative role of membrane skeleton and bilayer in the mechanical behaviour of red blood cells, Bioelectrochemistry 62 (2004) 107–113.